Electronic Supplementary Information for

Transparent PEDOT counter electrodes for bifacial dye sensitized solar cells with cobalt complex mediator

Yiming Li,[a] Jing Wang,[a] Hao Wang,[a] Zhichao Di,[a] Mingyan Liu,[a] Xueping Zong,[a] Chunsheng Li,[b] Yan Sun,[b] Mao Liang[a] and Zhe Sun[a] *

[a]*Tianjin Key Laboratory of Organic Solar Cells and Photochemical Conversion, School of Chemistry & Chemical Engineering, Tianjin University of Technology, Tianjin 300384, P. R. China.*

[b]*Key Laboratory of Advanced Electrode Materials for Novel Solar Cells for Petroleum and Chemical Industry of China, School of Chemistry and Life Sciences, Suzhou University of Science and Technology, Suzhou City, Jiangsu Province 215009, P. R. China*

Fax: +86-22-60214252

Tel: +86-22-60214259

E-mail: zhesun@tjut.edu.cn;

List of Contents

1. Experimental Section

1.1 Chemicals and materials

All the chemicals, including 3,4-ethylenedioxythiophene (EDOT, 97%, Sigma-Aldrich), sodium dodecyl sulfate (SDS, 98.5%, Aladdin), lithium bis(trifluoromethanesulfonyl)imide (Li-TFSI, 99.99%, Sigma-Aldrich), 4-*tert*-butylpyridine (4-TBP, Alpha), chloroplatinic acid ($H_2PtCl_6 \cdot 6H_20$, 99.95%, Sigma-Aldrich) and acetonitrile (AN, 99.9%, Energy Chemical) were used as received without further purification. A 18 nm TiO_2 particle paste (18NR-T) were purchased from Dyesol. Fluorine-doped tin oxide glass substrates (FTO, 7 and 14 Ω/square) were purchased from NSG Group. Sensitizer M22 (E)-2-cyano-3-(7-(4-((9,9-dipropyl-9H-fluoren-2-yl)(5,5,10,10,15,15-hexapropyl-10,15-dihydro-5H-di-indeno [1,2-a:1',2'-c]fluoren-2-yl)amino)phenyl)-2,3-dihydro-6H-cyclopenta[b][1,4] dioxin-5-yl)acrylic acid) were synthesized according to the reported methods.[1]

1.2 Fabrication of PEDOT counter electrodes

FTO glass substrate (7 Ω/square) was precleaned by sonicating in a bath of detergent, deionized water, and ethanol sequentially for 30 min. Electropolymerization was conducted with a three-electrode setup consisting of a FTO substrate as the working electrode, a Pt sheet as the counter electrode, and Ag/AgCl as the reference electrode. The electrolyte was prepared by dissolving 0.01 M EDOT monomer, 0.1 M Li-TFSI, and 0.07 M SDS into deionized water. The electropolymerization reaction was modulated with AC current signal generated by Zennium electrochemical workstation (Zahner, Germany) in galvanostatic mode. The AC current signal is triangular wave as described in eq S1,

$$i = \begin{cases} i_0 + i_{\mathrm{m}}\left(\dfrac{2t}{T} - 2n + \dfrac{1}{2}\right) & t \in \left[n - \dfrac{1}{2}, n\right]T \\ i_0 - i_{\mathrm{m}}\left(\dfrac{2t}{T} - 2n - \dfrac{1}{2}\right) & t \in \left[n, n + \dfrac{1}{2}\right]T \end{cases} \quad n = 0, 1, 2, \cdots \qquad \text{(S1)}$$

where i is the applied AC current, i_0 is the average of current, i_{m} is modulation amplitude, T is signal period, n is the number of cycles. During electropolymerization, AC current signal with the frequency of 5 Hz and modulation amplitude of 0.5 mA was applied to the three-electrode setup for 1-16 s. Poly(3,4-ethylenedioxythiophene) (PEDOT) deposited FTO substrate was subsequently immersed into 0.1 M SDS aqueous solution for 5 min. After that, PEDOT counter electrode was washed with deionized water and dried by air flow.

1.3 Fabrication of Pt counter electrodes

Platinized counter electrode was fabricated by spin-coating 5 mM isopropanol solution of H_2PtCl_6 onto FTO substrate (7 Ω/square) at 3000 rpm for 20 s. Then Pt deposited substrate was heated at 395 °C in an oven for 15 min.

1.4 Fabrication of photoelectrode and device assembly

TiO_2 photoanode was fabricated by using screen-printing technique. FTO-coated glass substrate (14 Ω/square) was precleaned with the procedure described in section 1.2. In brief, a blocking layer of TiO_2 was deposited by immersing FTO substrate into 40 mM aqueous $TiCl_4$ solution at 70°C for 30 min. The resultant FTO substrate was coated by TiO_2 colloid paste (18NR-T). After drying at 100 ^oC for 10 min, the TiO_2 coated FTO substrate was sintered at 500°C for 30 min. Then TiO_2 film was soaked in the $TiCl_4$ solution for another 30 min. It is followed by sintering at 500°C for 30 min.

Dye sensitization was carried out by immersing the TiO_2 film into 300 μM dichloromethane/ anhydrous ethanol (v/v=1:4) solution of an organic dye M22 for 30 h. The sensitized film was rinsed with anhydrous ethanol, and dried by air flow. The TiO_2 photoanode was assembled with counter electrode by using a 25 μm Surlyn hot-melt gasket (Solaronix, Switzerland) serving as spacer and seal. Electrolyte based on cobalt complex was perfused into the assembly via vacuum backfilling. The composition of cobalt complex based electrolyte is 0.25 M $[Co(II)(phen)_3]$ $(TFSI)_2$, 0.05 M $[Co(III)(phen)_3](TFSI)_3$, 0.1M Li–TFSI, and 0.5 M 4–tertpyridine (TBP) in acetonitrile.

1.5 Fabrication of dummy cells

Symmetrical sandwich dummy cell was fabricated from two identical FTO substrates which were separated by 45 μm thick Surlyn hot-melt gasket (Solaronix, Switzerland) as a sealant and spacer. The gasket is annular-shape leaving an active area of 0.283 cm^2. The distance between electrodes was determined by a digital micrometer, which revealed the average distance was (30 ± 2) μm. According to the suggestions by Kavan et al., the measured current densities in cyclic voltammograms were corrected by a coefficient of 30/δ, where δ is the measured thickness (in μm) of the actual dummy cell.[2] Such correction is necessary to avoid small sample-to-sample variations in device thicknesses and hence make the electrochemical data comparable. The cell was filled with the electrolyte through a hole in one FTO substrate which was finally closed by a 45 μm thick Surlyn seal. The composition of cobalt complex

based electrolyte is 0.25 M [Co(II)(phen)$_3$] (TFSI)$_2$, 0.05 M [Co(III) (phen)$_3$](TFSI)$_3$, and 0.1 M Li–TFSI in acetonitrile.

1.5 Measurements and characterizations

The morphologies of PEDOT counter electrodes (CEs) were measured by a MERLIN Compact field-emission scanning electron microscopy (SEM, Zeiss, Germany). Particle size distribution and surface coverage of PEDOT aggregates were determined based on the SEM images by using the Nano Measurer software. Atomic force microscope (AFM) images are obtained by using Dimension Icon (Bruker, USA), and the root mean square of R_q was determined. Film thickness was obtained by a DektakXT profilometer (Bruker, Germany). XPS analyses were conducted by using a K-alpha X-ray photo-electron spectrometer (ThermoFisher, USA) with an Al-Kα (1486.6 eV) achromatic X-ray source. The Raman spectra were measured using a Raman spectrometer (Evolution, Horiba Scientific) equipped with 532 nm laser. Specular transmittance spectra of the PEDOT counter electrodes and Pt counter electrodes were determined by using a UV-2600 spectrophotometer (Shimadzu, Japan).

Electrochemical impedance spectra (EIS) of the dummy cells were collected by a Zennium electrochemical workstation (Zahner, Germany). Scanning frequency ranges from 100 kHz to 0.5 Hz, and modulation amplitude was set to 10 mV. Tafel polarization curves of the symmetrical dummy cells were determined from with a scan range from −1.0 to +1.0 V at a resolution of 10 mV. Electrochemical stability test was conducted using Zennium electrochemical workstation. Dummy cells were aged by performing cyclic voltammetry sweeping between -1 V and 1 V for three times. This is followed by the impedance measurement shown above. After repeating such procedure for 9 times, electrochemical stability of the dummy cells was characterized by fitting the EIS spectra determined in each step. Current-voltage (*J*–*V*) characteristics were measured with a computer controlled Keithley-2400 digital source meter (Keithley, USA). A solar simulator equipping with a 450 W xenon lamp and an AM 1.5 filter (Oriel 91160-1000, Newport, USA) was employed as the light source. The illumination intensity was adjusted to 1 sun (100 mW cm^{-2}) by using a NREL-calibrated Si solar cell. In the measurement in standard test conditions, *J*–*V* curves were determined with monofacial irradiation on the front side of the DSCs. In the measurement of power production of the bifacial DSCs, a test setup was utilized for modelling the realistic illumination conditions. As shown in Fig. S, the setup splits the simulated sunlight (AM 1.5, 100 mW cm^{-2}) into two beams. One is

irradiated at the front side of DSC with a reflection mirror. The other is attenuated by a series of neutral density filters (NDF) before irradiated on the rear side of DSC.

2. AC current signals and voltage responses during electropolymerization

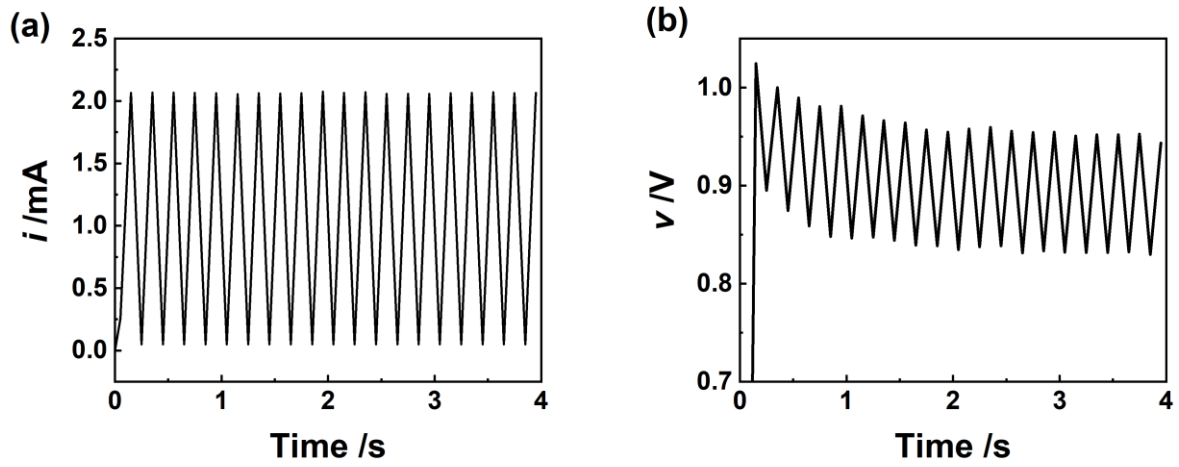

Fig. S1 Current-voltage evolution in electropolymerization reaction. (a) AC current, (b) voltage response.

3. XPS spectra of PEDOT deposited on FTO sheet

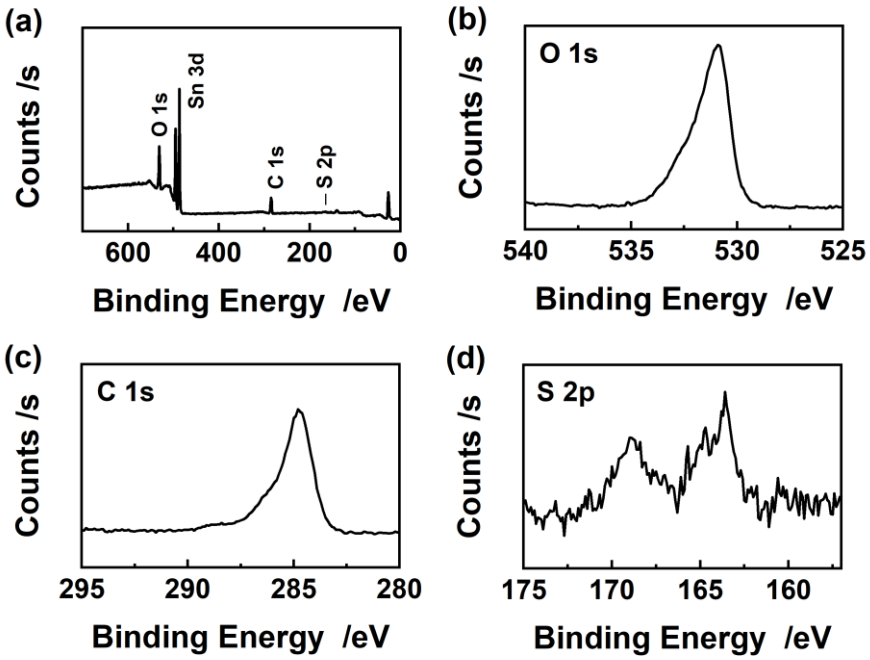

Fig. S2 XPS spectra of PEDOT deposited on FTO sheet. (a) Survey in whole B.E., (b) O 1s, (c) C 1s, (d) S 2p core-level survey.

4. Raman spectrum of PEDOT deposited on FTO sheet

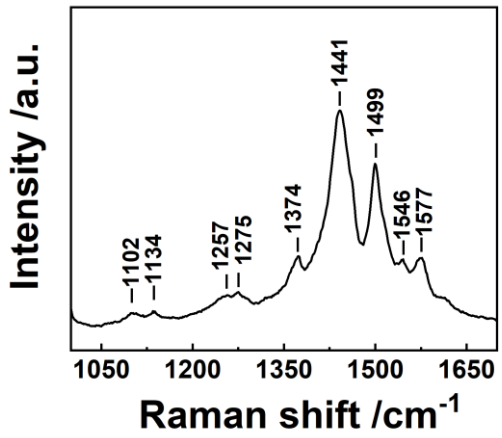

Fig. S3 Raman spectrum of PEDOT deposited on FTO sheet.

5. SEM images of PEDOT counter electrodes

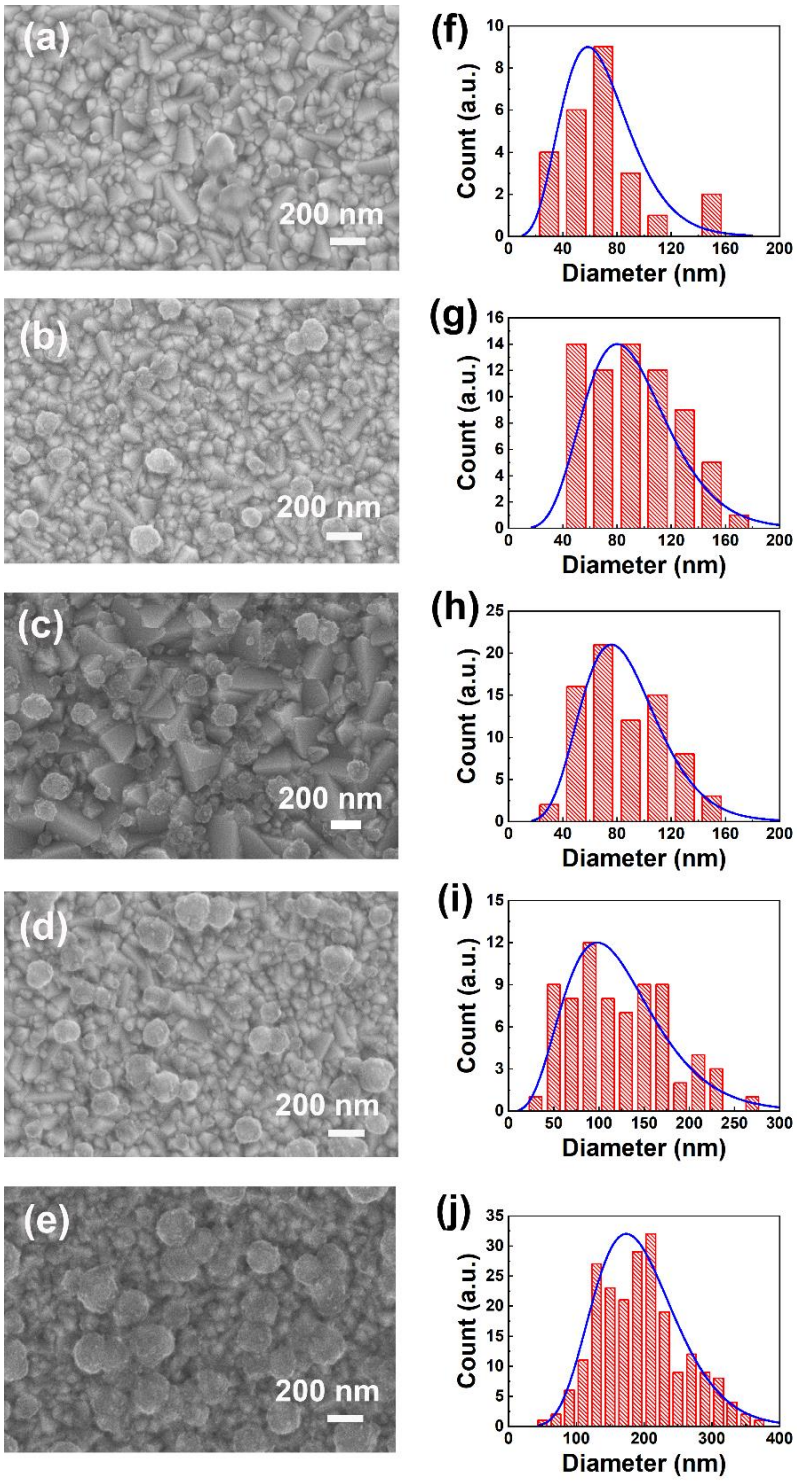

Fig. S4 Top view of the SEM images of PEDOT counter electrodes fabricated with different electropolymerization time: (a) 1 s, (b) 2s, (c) 4 s, (d) 8 s, (e) 16 s. The corresponding size distribution of the PEDOT aggregates are indicated in the images f, g, h, i, and j, respectively.

6. Magnified AFM image of PEDOT deposited on FTO sheet

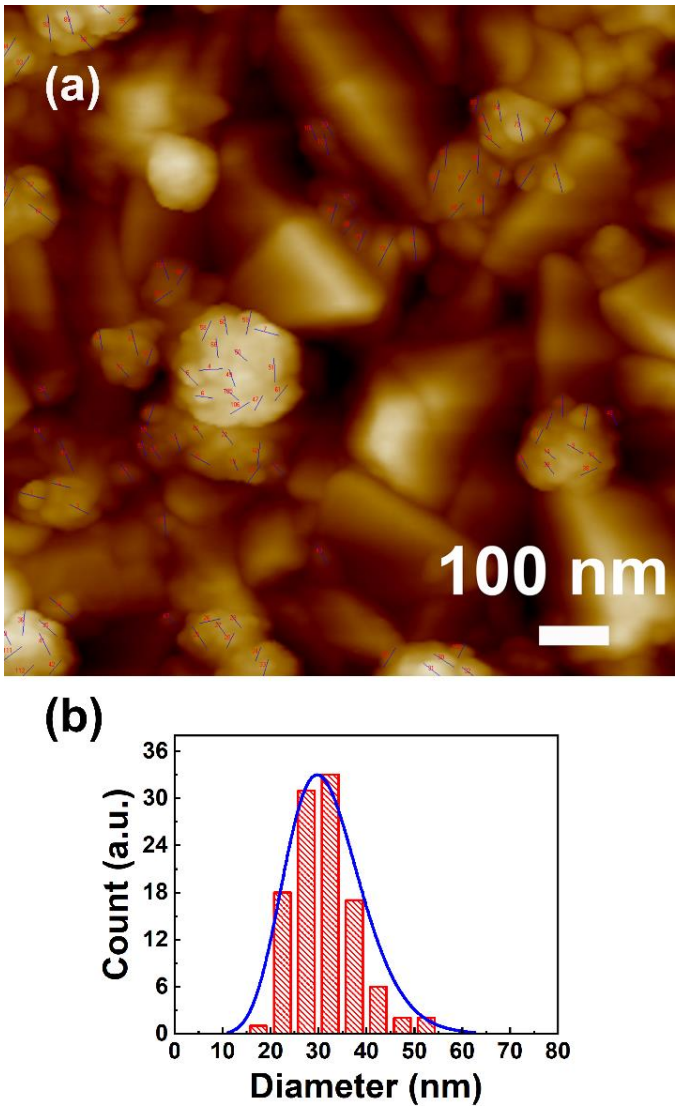

Fig. S5 (a) AFM image of the PEDOT deposited on FTO sheet. The blue lines indicate the sampling of PEDOT particles in the hierarchical structure. (b) Size distribution of the PEDOT particles.

7. A model for predicting the coverage of PEDOT

A model is established herein to predict the variation of PEDOT coverage during the electropolymerization reaction. As depicted schematically in Fig. S6, the electropolymerization reaction can be described as follows. (1) Colloidal EDOT particles with negative charges are drifted to the surfaces of bare FTO in response to the applied electric field. (2) Electropolymerization occurs in the EDOT "pools". Colloidal EDOT particles are converted into solid PEDOT particles, and the SDS molecules depart from the surface of the PEDOT particles and diffuse back to the aqueous solution. The PEDOT particles anchoring on the FTO surface are called PEDOT "seeds". (3) The anchored PEDOT seeds continue to grow via electropolymerization, which gives rise to the formation of the PEDOT aggregates.

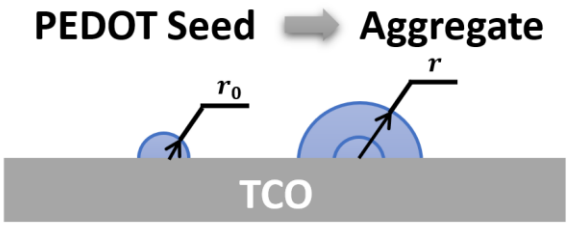

Fig. S6 Schematic of the PEDOT seed and aggregate in the electropolymerization reaction.

To simplify the model, the electropolymerization is supposed to occur on a flat TCO surface. The concentration of colloidal EDOT particles (c_{EDOT}) is large enough to make the TCO surface and the PEDOT aggregates electrostatic-screened. Thereby c_{EDOT} is independent of the position perpendicular to the TCO surface. The generation rate of the PEDOT "seeds" in the electropolymerization is related to area of the bare TCO surface,

$$\frac{\mathrm{d}n_0(t)}{\mathrm{d}t} = k_{\mathrm{TCO}} c_{\mathrm{EDOT}} [S_{\mathrm{TCO}} - S_{\mathrm{cov}}(t)] \qquad \text{(S1)}$$

where $n_0(t)$ is the number of the PEDOT "seeds" at the reaction time of t, S_{TCO} is the area of TCO surface, $S_{\mathrm{cov}}(t)$ is the area of PEDOT occupied surface at the reaction time of t, and k_{TCO} is rate constant of the electropolymerization reaction at TCO surface.

As shown in Fig. S6, PEDOT "seed" is semi-sphere with the diameter of r_0. For simplicity, the growth of PEDOT "seed" only results in the increase of diameter, does not affect the semi-sphere shape. A low coverage of PEDOT aggregates is assumed also. It means the PEDOT aggregates grow independently, which can also be regarded as semi-spheres. In line with this assumption, the invariant c_{EDOT} allows the diameter of PEDOT aggregates (r) to increase linearly with the reaction time,

$$\frac{\mathrm{d}r}{\mathrm{d}t} = k_{\mathrm{p}} \tag{S2}$$

where k_{p} is rate constant of the reaction occurring at the surface of PEDOT aggregates. According to eq S2, the PEDOT "seed" generated at the time t' grows to the diameter of r with the reaction time of t, that is

$$r = k_{\mathrm{p}}(t - t') + r_0 \tag{S3}$$

Surface area that the PEDOT aggregate with the diameter of r covers ($S_{\mathrm{p,r}}$) is written as

$$S_{\mathrm{p,r}}(t, t') = \pi\left[k_{\mathrm{p}}(t - t') + r_0\right]^2 \tag{S4}$$

Therefore, the total area that the PEDOT aggregates covering (S_{cov}) at the reaction time t is given by

$$S_{\mathrm{cov}}(t) = \int_0^t S_{\mathrm{p,r}}(t, t')\frac{\mathrm{d}n_0(t')}{\mathrm{d}t'}\mathrm{d}t' \tag{S5}$$

By inserting eq S1 into eq S5, one obtains the following expression,

$$S_{\mathrm{cov}}(t) = \int_0^t \pi k_{\mathrm{TCO}} c_{\mathrm{EDOT}}\left[k_{\mathrm{p}}(t - t') + r_0\right]^2 [S_{\mathrm{TCO}} - S_{\mathrm{cov}}(t)]\mathrm{d}t' \tag{S6}$$

The integral equation S6 is then converted into its differential form,

$$\frac{\mathrm{d}S_{\mathrm{cov}}(t)}{\mathrm{d}t} = \pi r_0^2 k_{\mathrm{TCO}} c_{\mathrm{EDOT}}[S_{\mathrm{TCO}} - S_{\mathrm{cov}}(t)] \tag{S7}$$

This equation is solved analytically. And the solution is given by

$$\ln\frac{S_{\mathrm{TCO}} - S_{\mathrm{cov}}(t)}{S_{\mathrm{TCO}}} = -\pi r_0^2 k_{\mathrm{TCO}} c_{\mathrm{EDOT}} t \tag{S8}$$

The time dependent surface coverage of the PEDOT aggregates (η_{cov}) is defined as

$$\eta_{\mathrm{cov}}(t) = \frac{S_{\mathrm{cov}}(t)}{S_{\mathrm{TCO}}} \tag{S9}$$

According to eq S7, $\eta_{\mathrm{cov}}(t)$ is given by

$$\eta_{\mathrm{cov}}(t) = 1 - \exp(-\pi r_0^2 k_{\mathrm{TCO}} c_{\mathrm{EDOT}} t) \tag{S10}$$

Eq S10 indicates that a semilogarithmic relationship with$1 - \eta_{\mathrm{cov}}(t)$ and the reaction time. Fig. S7 indicates that the semilogarithmic relation is verified according to the experimental results.

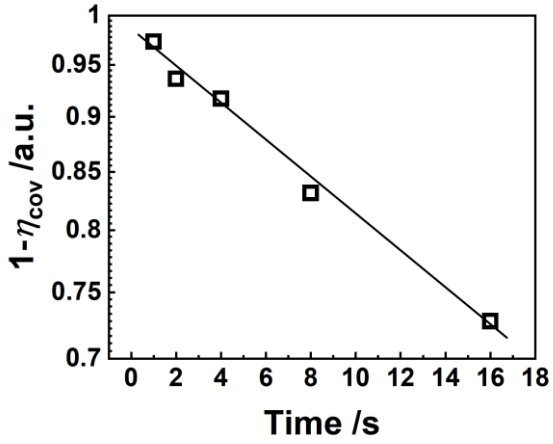

Fig. S7 Semilogarithmic plot of surface coverage versus the electropolymerization reaction time.

8. Photographs of the counter electrodes

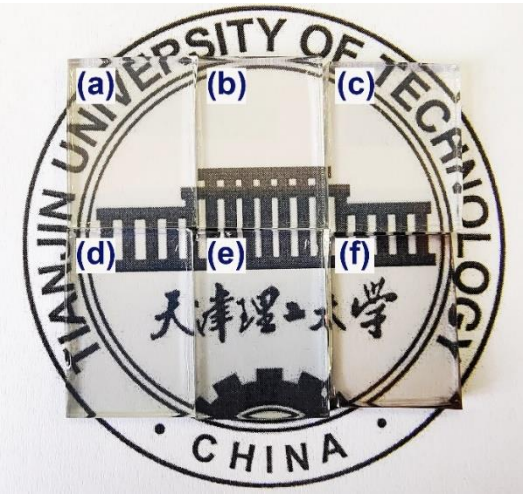

Fig. S8 Photographs of PEDOT based counter electrodes. (a) P-1s, (b) P-2s, (c) P-4s, (d) P-8s, (e) P-16s, (f) Pt.

9. Schematic of symmetrical dummy cell and equivalent circuit for impedance curve fitting

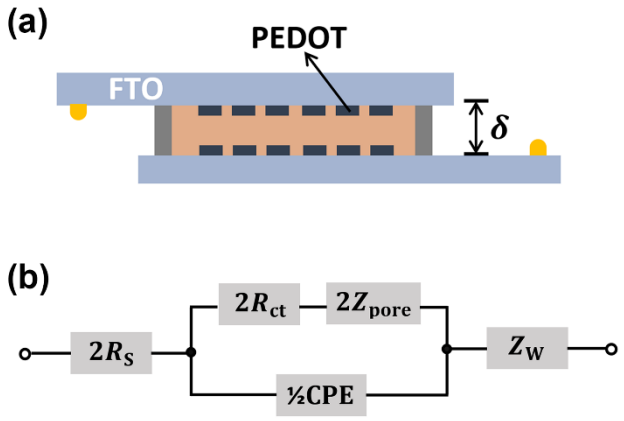

Fig. S9 (a) Schematic of symmetrical dummy cell with PEDOT CEs. (b) Equivalent circuit for fitting the impedance spectra.[2] In the equivalent circuit, R_{ct} is the charge transfer resistance, CPE is the constant phase capacitance at counter electrode/electrolyte interface, Z_{pore} is the Nernst diffusion impedance in porous layer, Z_w is the Warburg element and R_s is the series resistance.

10. Effect of charge transfer resistance on CE transmittance and the density of current loss

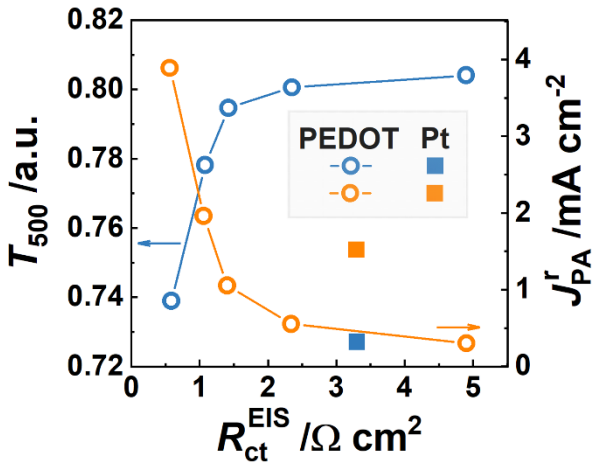

Fig. S10 Plots of transmittance of the CEs at 500 nm (T_{500}) and $J_{PA}{}^{r}$ (300 nm - 900 nm) versus charge transfer resistance ($R_{ct}{}^{EIS}$) of PEDOT CEs. The values of Pt CE are marked for comparison.

11. Cycling stability of counter electrodes

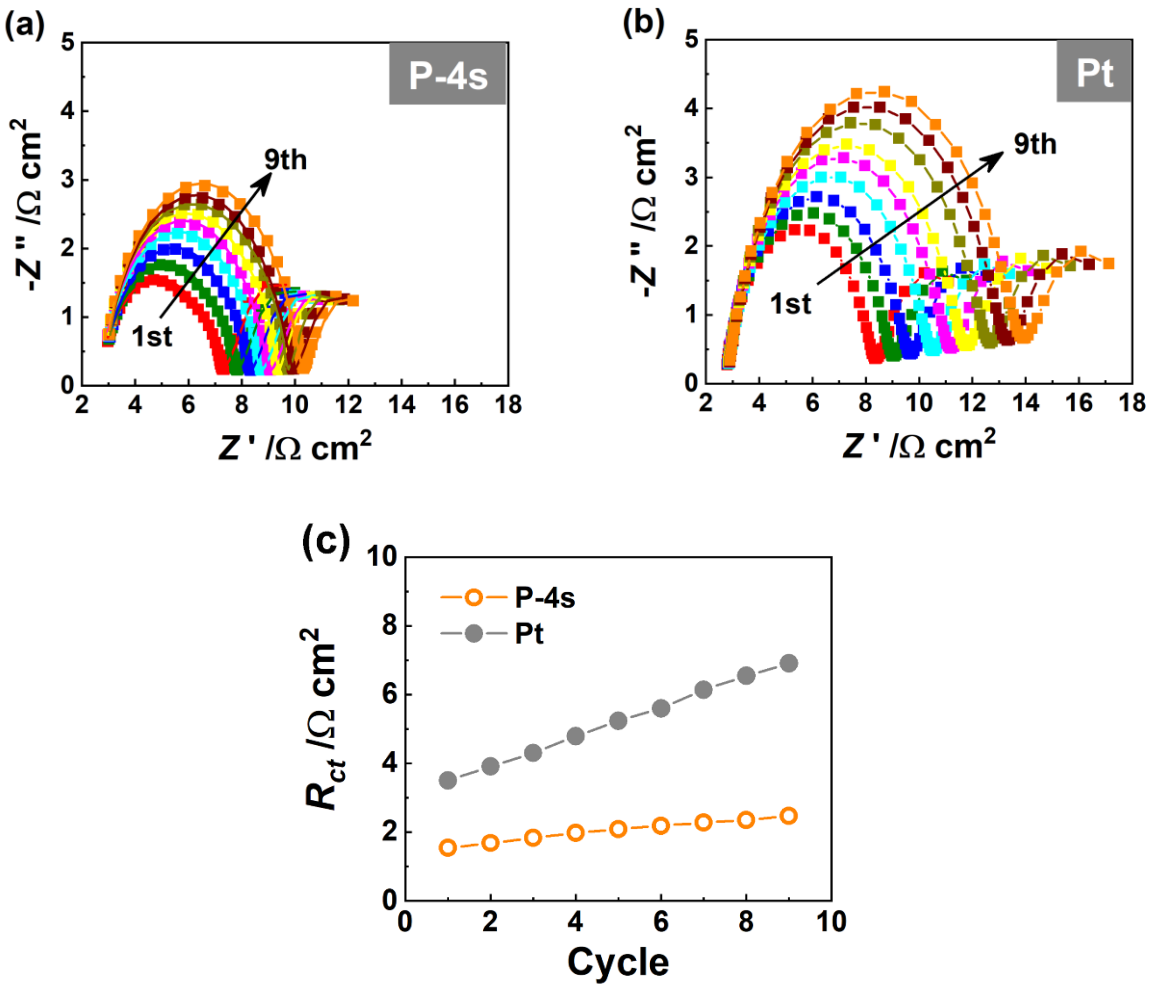

Fig. S11 Nyquist spectra of cycling stability of symmetrical dummy cells based on (a) P-4s CE and (b) Pt CE. Solid lines indicate the best fits based on the equivalent circuit shown in Fig. S9b. (c) Variations of R_{ct}^{EIS} in the symmetrical dummy cells with P-4s CE and Pt CE in response to cyclic voltammetry scans.

12. Molecular structure of dye M22

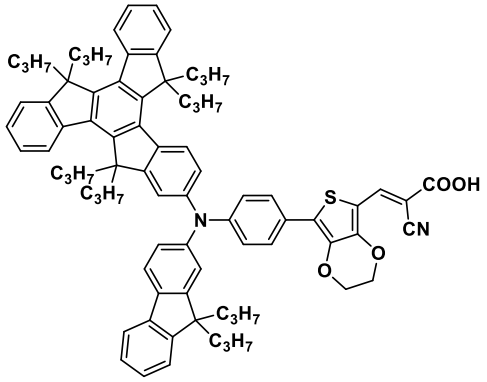

Fig. S12 Molecular structure of dye M22.

13. Photographs of the bifacial DSCs

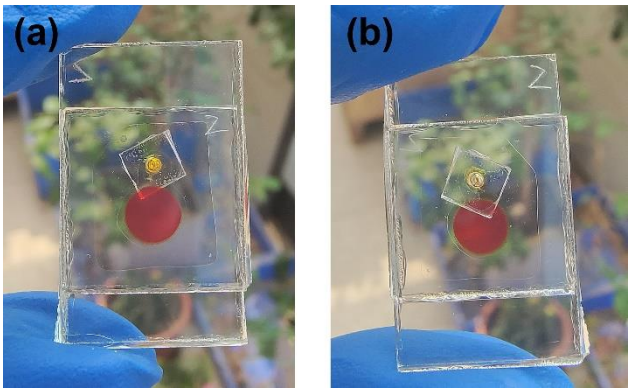

Fig. S13 Photographs of bifacial dye sensitized solar cells based on P-4s counter electrodes. (a) front side (b) rear side.

14. Schematic of power production test in simulated realistic conditions

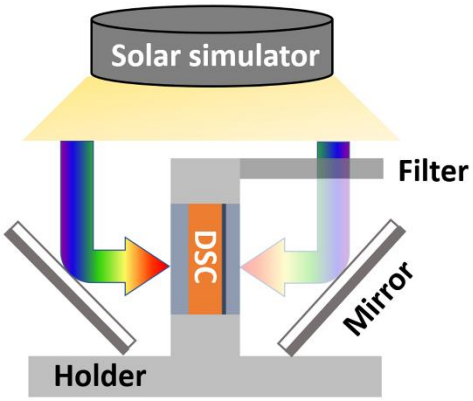

Fig. S14 Schematic test setup in the characterization of bifacial DSC.

15. Power production of the bifacial DSCs in realistic test conditions

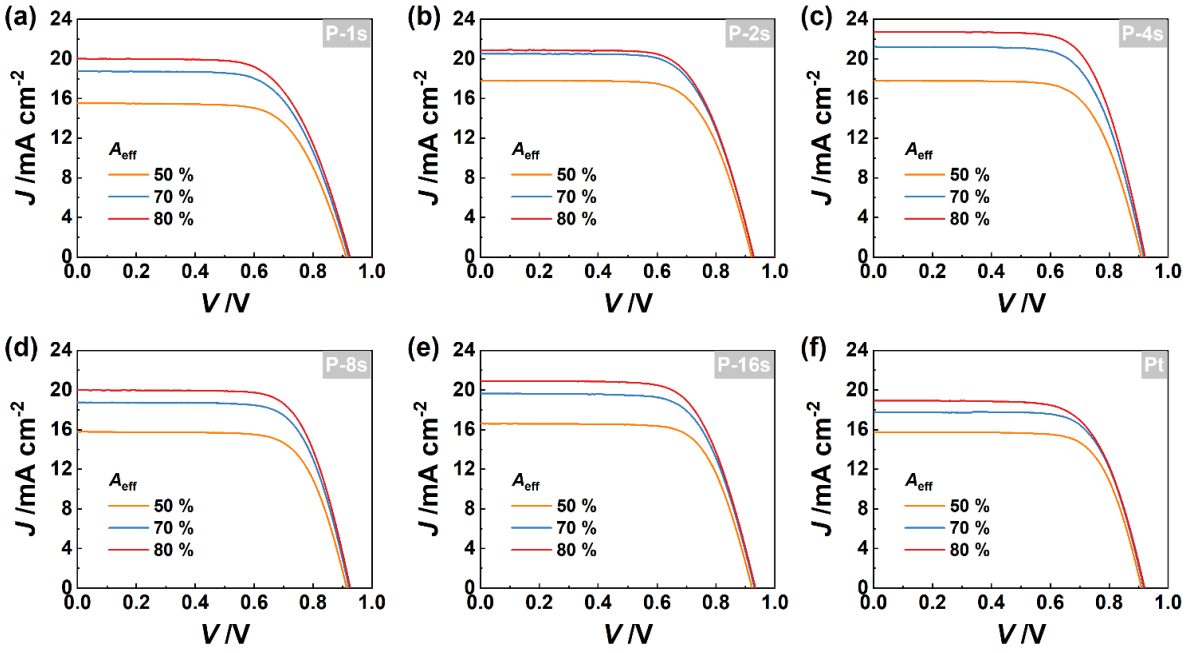

Fig. S15 J-V characteristics of the bifacial DSCs with various counter electrodes under realistic test conditions. (a) P-1s, (b) P-2s, (c) P-4s, (d) P-8s, (e) P-16s, (f) Pt.

Table S1. Photovoltaic parameters of the bifacial DSCs in realistic test conditions [a]

Cell	A_{eff} /%	V_{oc} /mV	J_{sc} /mA cm^{-2}	OPD/ mW cm^{-2}	FF
P-1s	50	913	15.51	9.52	0.67
	70	921	18.74	11.2	0.65
	80	926	20.02	11.9	0.64
P-2s	50	921	17.78	11.3	0.69
	70	928	20.51	12.8	0.67
	80	929	20.85	13.0	0.67
P-4s	50	910	17.78	11.2	0.70
	70	918	21.21	13.3	0.68
	80	922	22.72	14.5	0.69
P-8s	50	915	15.78	10.3	0.71
	70	923	18.73	12.2	0.71
	80	927	19.98	13.0	0.70
P-16s	50	923	16.60	10.9	0.71
	70	931	19.63	12.5	0.69
	80	934	20.90	13.3	0.68
Pt	50	913	15.51	9.52	0.67
	70	921	18.74	11.2	0.65
	80	926	20.02	11.9	0.64

[a]The active area of the DSCs is 0.16 cm^2. V_{oc}: open circuit voltage, J_{sc}: short circuit current density, OPD: output of power density, FF: fill factor, A_{eff}: effective albedo.

16. Bifacial gain of energy of the DSCs

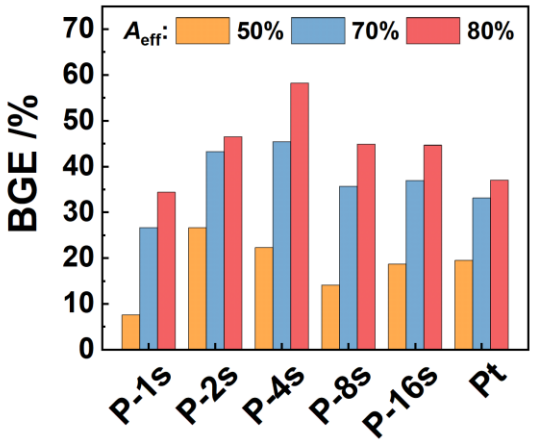

Fig. S16 Bifacial gain of energy of the DSCs based on PEDOT CEs and Pt CE. Effective albedo (A_{eff}) is indicated in the image.

References

1. Y. Hao, M. Liang, Z. Wang, F. Cheng, C. Wang, Z. Sun and S. Xue, *Tetrahedron*, 2013, **69**, 10573-10580.
2. L. Kavan, J. H. Yum and M. Gratzel, *Nano Lett.*, 2011, **11**, 5501-5506.